Grattan, K. T., Agrawal, A., Kejalakshmy, N. & Rahman, B. M. (2009). Soft Glass Equiangular Spiral Photonic Crystal Fiber for Supercontinuum Generation. IEEE Photonics Technology Letters, 21(22), 1722 - 1724. doi: 10.1109/LPT.2009.2032523 <http://dx.doi.org/10.1109/LPT.2009.2032523>

Soft Glass Equiangular Spiral Photonic Crystal Fiber for Supercontinuum Generation

Arti Agrawal, *Member, IEEE,* N. Kejalakshmy, B. M. A. Rahman *Senior Member, IEEE*

and K. T. V. Grattan

Abstract— An Equiangular Spiral Photonic Crystal Fiber (ES-PCF) design in soft glass is presented that has high nonlinearity (γ>5250 $W^{-1}.km^{-1}$ at 1064*nm* and γ>2150 $W^{-1}.km^{-1}$ at 1550*nm*) with a low and flat dispersion (D~0.8 *ps/km.nm* and Dispersion slope ~-0.7*ps/km.nm*^{2} at 1060*nm*). The design inspired by nature is characterized by a full-vectorial finite element method. The ES-PCF presented improves over the mode confinement of triangular core designs and dispersion control of conventional hexagonal PCF, combining the advantages of both designs; it can be an excellent candidate for generating supercontinuum (SC) pumped at 1.06μm.

***Index Terms*- Equiangular spiral (ES), finite element method, photonic crystal fiber (PCF), Supercontinuum Generation (SCG).**

I. Introduction

Photonic Crystal fibers (PCF), with a microstructure of air holes around a solid central core, guide light through modified total internal reflection. Tailoring the air hole arrangement can yield properties such as anomalous dispersion at wavelengths shorter than the zero material dispersion wavelength. It is possible to obtain a tightly confined optical mode with small effective area and large non-linearity which coupled with flat, anomalous dispersion has led to successful broadband Supercontiuum Generation (SCG) in PCF [1].

At present, expensive and bulky Ti-sapphire laser sources are used to pump SCG. Replacing these by Yb doped fiber laser sources has the potential to make SC systems more compact and inexpensive. Therefore much effort has been expended to generate SC pumped at 1.06μm by Yb doped fiber laser cavities. One aspect of the effort is to increase γ in the PCF ($\gamma = 2\pi n_2 / \lambda A_{eff}$, by decreasing A_{eff}; where A_{eff} : effective area, n_2 : Kerr non-linear coefficient, or by increasing n_2). The Kerr nonlinear coefficient in silica limits the maximum possible γ in conventional PCF. Soft glasses, however, offer higher refractive indices and n_2 values than silica and lower processing temperatures that allow fabrication through extrusion. These developments have led to extensive research on PCF in compound glasses [2-8]. Design optimization to increase γ has led to designs such as tapered PCF similar to nano-wires [7] and Triangular Core fibers (TC) [6] that are the closest approximation to jacket Air-Suspended Rod (ASR) fibers [9]. The ASR design has the smallest possible A_{eff} (largest γ) however, it is a theoretical concept and in practice TC fibers are the closest in design and performance to ASR that can be fabricated, and we shall compare our results with those for TC fibers. Nano-wires [7] have the issues of mechanical stability and collapse of air-holes during fabrication. While in the TC [6] fibers decrease in core size beyond a certain point leads to decrease in γ as the mode does not remain confined within the core. For such designs some of the highest values of γ reported in the literature lie in the range ~2000-2200 $W^{-1}.km^{-1}$ at 1550*nm* for core diameters in the range 0.6-1.0 μm [6,8].

Lead silicate glasses exhibit good thermal and crystallisation stability, with the highest γ exhibited by SF57. Therefore this letter focuses on PCF design with commercially available Schott SF57 glass for SCG. In the literature the highest γ reported in SF57 glass PCF is ~1860 $W^{-1}.km^{-1}$ 1550*nm* for core diameter ~0.95 μm [6]. The same group has also reported a PCF with core diameter~1.3μm and a Zero Dispersion Wavelength (ZDW)~1.06μm and dispersion slope~1*ps/nm*^{2}*.km* [6]. In this letter the ES-PCF design exhibits γ>5250 $W^{-1}.km^{-1}$ at 1064*nm* (γ > 2150 $W^{-1}.km^{-1}$ at 1550nm). In addition, the ES-PCF design has a flat dispersion at 1060 nm with D~0.795 *ps/nm.km*.

II. Equiangular PCF Design

Figure 1 shows the air-hole arrangement in the ES-PCF design, which mimics the 'spira mirabilis' (Equiangular Spiral-ES) and appears in nature in nautilus shells and sunflower heads. It leads to efficient feature growth/packing of seeds and the growth of this type of curve does not alter the shape of the curve. In the ES-PCF, each arm of air holes forms a single ES of radius r_o, angular increment θ, and the radius of each air hole is fixed (r). In the ES, the radii drawn at any equal intervals of θ are in a geometric progression, therefore, the pitch (distance between air holes) in a ring increases with the ring number. The design therefore has several parameters to optimize γ and dispersion. In addition, a small defect air-hole with radius r_c is introduced at the centre of the structure to flatten the dispersion [10]. We expect that the ES-PCF can be fabricated by the new extrusion techniques that are being

Manuscript received April 22, 2009. Authors are with the School of Engineering and Mathematical Sciences, City University London, EC1V 0HB, UK (phone: 207-040-8123; fax: 207-040-8568; e-mail: b.m.a.rahman@city.ac.uk, arti.agrawal.1@city.ac.uk).

applied to realise challenging structures in soft glass such as nano-wires [7] and TC fibers [6].

A full-vectorial finite element method [11] has been used to characterize the ES-PCF design. About 43944 second order triangular elements arranged in an irregular mesh have been used to represent the structure. A single simulation run on a 64 bit quad-core Intel Pentium desktop computer took about 60s. Results are reported for two optimized structures with 7 arms, 4 rings, r_o=*0.525 μm, θ=26°*, (Design A: *r=0.1375 μm,* r_c ~34*nm)* and (Design B: *r* is same as Design A, except for the third ring where *r=0.125μm,* r_c~20*nm,).* The minimum hole-to-hole separation is 130*nm* for A (average value~750*nm*) and 180*nm* for B (average value~760*nm*) while in TC fibers the fine struts that support the core have thickness < 250nm [6]. In computing the dispersion of the ES-PCF, material dispersion has been taken into account by using the Sellemeier equation to generate the refractive index of SF57 at different wavelengths; in computing γ for the ES-PCF, $n_2 = 4.1\times10^{-19} m^2/W$ has been used similar to [6]. A_{eff} calculations are based on the definition in [12].

III. Results

Table 1 shows the γ and A_{eff} values for the ES-PCF with varying r_c at operating wavelengths of 1550*nm* and 1064*nm*. First we note that if the number of elements is increased from 43944 to162508, the A_{eff} values (for the case r_c ~0*nm,* Design A) do not change, this indicates convergence and the mesh with 43944 elements gives sufficient accuracy. The maximum γ value is attained when the defect hole is not present in the structure (Design A {Design B}: 5583 {5558} $W^{-1}.km^{-1}$ at 1064*nm* and 2307 {2205} $W^{-1}.km^{-1}$ at 1550*nm*). However, even with the defect air hole (~34*nm* for *A* and 20*nm* for *B*) a very large γ~5261{5426} $W^{-1}.km^{-1}$ at 1064*nm* and γ> 2150 {2155} $W^{-1}.km^{-1}$ at 1550*nm* are obtained. These values are much larger than 1860 $W^{-1}.km^{-1}$ at 1550*nm* reported so far [6,8] and exceed the maximum limit of γ values for PCF with similar core diameters. The TC geometry usually provides the smallest possible A_{eff} (largest γ) therefore, the ES-PCF yielding a larger γ (than the corresponding TC) is unexpected.

This surprising result is an outcome of the fact that in the ES-PCF each ring of air holes is rotated with respect to the previous one, therefore the outer air holes block the field from escaping into glass regions which the previous ring could not effectively stop (see Fig. 2a). Furthermore, the design has several parameters (angular increment of each spiral arm, number of spiral arms and rings, size of air holes) to optimize the location of air holes for field confinement which are not present in TC designs. For a TC design in a particular material, there is a minimum core size (core diameter d_{min}) beyond which further decrease leads to cut off and the field expands rapidly leading to a large A_{eff} and small γ [8]. The ES-PCF design offers the potential to find a set of spiral parameters to get smaller A_{eff} than the TC fiber for values of the core diameter that are comparable or smaller than d_{min}. For operation at 1550nm, the ES-PCF A_{effmin}~0.710 μm^2 and for operation at 1064nm A_{effmin}~0.347 μm^2 which is smaller than the A_{effmin} in the TC fiber [6].Therefore, the ES-PCF design has efficient air hole packing which provides superior field confinement compared to the TC design. In addition, the ES-PCF design also provides better control over dispersion than the TC design.

Tailoring the dispersion to achieve flat, anomalous dispersion with small slope and a zero crossing near/at the pump wavelength is an extremely important aspect in SC generation in PCF [13]. Design engineering has to be performed to balance the effects of enhancing non-linearity and flattening dispersion. The optimized ES-PCF has low (Design A{Design B}: D~0.795{0} *ps/nm.km)* and flat dispersion at 1.06 *μm* (dispersion slope ~-0.751{-0.9}*ps/nm².km at* 1.06 *μm*). This dispersion is smaller and flatter than the values possible with present state of the art TC design [6]. In TC designs due to small core and large index contrast, the effective modal index of the guided mode changes rapidly with wavelength, yielding large dispersion slope that can be difficult to flatten with the limited number of design parameters. Conventional PCF designs can allow for better dispersion control through engineering of the cladding microstructure, but with lower non-linearity. However, the ES-PCF can simultaneously yield large non-linearity with flat and small, anomalous dispersion.

Figure 3 shows the dispersion variation of the ES-PCF with wavelength (as r_c is varied) with and without the central defect air-hole. The ES-PCF without the defect air-hole (dash-dot line) has normal dispersion in the entire range visible in Fig. 3 all though the dispersion peaks close to zero at λ~1.0 *μm*. At the short wavelength end the dispersion increases with wavelength as the field spreads in the central glass region and effective index (n_{eff}) decreases rapidly due to the field interacting with the first ring of air-holes (see, Fig. 2a). As the field spreads out farther and interacts with the glass in the region beyond the first ring of air-holes, the change in n_{eff} slows down and dispersion becomes somewhat flat (λ~1.0 *μm).*With further increase in wavelength, the field sees the influence of the second ring of air-holes (see Fig. 2b) which accelerates the change in n_{eff} and leads to large normal dispersion.

The defect hole compensates for the material dispersion [10] since the field in the central core region enters the defect hole and interacts with air. A larger size of the defect air-hole pushes the flat dispersion region towards more negative values. Thus by optimizing the size of the defect hole it is possible to obtain very flat dispersion near the pump wavelength of 1.06 *μm* for pumping SCG.

IV. Conclusions

In conclusion a novel Equiangular Spiral PCF (ES-PCF) design in SF57 glass has been presented that has high non-linearity γ>2150 $W^{-1}.km^{-1}$ at 1550*nm* and γ>5250 $W^{-1}.km^{-1}$ at 1064*nm*) which exceeds the maximum γ values possible in existing PCF designs. Also, the ES-PCF has low and flat dispersion with D~0.8 *ps/km.nm* and Dispersion slope ~-0.7*ps/km.nm²* at 1060*nm*. This design achieves large non-linearity along with very flat dispersion that can be tailored according to requirements. It combines the advantage of better dispersion control (seen in hexagonal PCF) which is not

possible with triangular core geometry with smaller A_{eff} and higher γ (better or similar to TC designs).The ES-PCF is extremely well suited for SCG pumped at 1.06μm.

REFERENCES

1. J.K. Ranka, R.S. Windeler and A.J. Stentz, "Visible continuum generation in air-silica microstructure optical fibers with anomalous dispersion at 800nm," *Opt. Lett.*, Vol. 25, no. 1, pp. 25-27, 2000.
2. T. M. Monro, Y. D. West, D. W. Hewak, N. G. R. Broderick, and D. J. Richardson, "Chalcogenide holey fibers," *Electron. Lett.*, vol. 36, no. 24, pp. 1998–2000, 2000.
3. V. Kumar, A. K. George, J. C. Knight, and P. S. Russell, "Tellurite photonic crystal fiber," *Opt. Exp.*, vol. 11, no. 20, pp. 2641–2645, 2003.
4. H. Ebendorff-Heidepriem, P. Petropoulos, S. Asimakis, V. Finazzi, R. C. Moore, K. Frampton, F. Koizumi, D. J. Richardson, and T. M. Monro, "Bismuth glass holey fibers with high nonlinearity," *Opt.Exp.*, vol. 12, no. 21, pp. 5082–5087, 2004.
5. H. Ebendorff-Heiderpriem, Y. Li and T.M. Monro, "Reduced loss in extruded soft glass microstructured fiber," *Electron. Lett.*, vol. 43, no. 24, pp. 1343-1344, 2007.
6. J. Y. Y. Leong, P. Petropoulous, J. H. V. Price, H. Ebendorff-Heiderpriem, S. Asimakis, R. C. Moore, K. Frampton, V. Finazzi, X. Feng, , T. M. Monro, and D. J. Richardson, "High-nonlinearity dispersion-shifted lead-silicate holey fibers for efficient 1-μm pumped supercontinuum generation," *Jrnl. Lightwav. Technol.*, Vol. 24, no. 1, pp. 183-190, 2006.
7. N.A. Wolchover, F. Luan, A.K. George, J.C. Knight and F.G. Omenetto, "High nonlinearity glass photonic crystal nanowires," *Opt. Exp.*, vol. 15, no. 3, pp. 829-833, 2007.
8. H. Ebendorff-Heiderpriem, P. Petropoulos, V. Finazzi, S. Asimakis, J. Y. Y. Leong, F. Koizumi, K. Frampton, R.C. Moore, D. J. Richardson, T. M. Monro, "Heavy metal oxide glass holey fibers with high nonlinearity," presented at the Optical Fiber Communication Conference and Exposition, March 6-11, 2005 , Anaheim, (Cal.), paper OThA3.
9. V. Finazzi, T. M. Monro and D. J. Richardson, "Small-core silica holey fiber: nonlinearity and confinement loss trade-offs," Jrnl. Opt. Soc. Amer. B, vol. 20, no. 7, pp. 1427-1436, 2003.
10. K. Saitoh, N. Florous and M. Koshiba, "Ultra-flattened chromatic dispersion controllability using a defected-core photonic crystal fiber with low confinement losses," *Opt. Exp.*, vol. 13, no. 21, pp. 8365-8371, 2005.
11. N. Kejalakshmy, B. M. A. Rahman, A. Agrawal, T. Wongcharoen and K. T. V. Grattan, "Characterization of single-polarization single-mode photonic crystal fiber using full-vectorial finite element method," *App. Phys. B*, vol. 93, no. 1, pp. 223-230, 2008.
12. G. P. Agrawal, *Nonlinear Fiber Optics*, Academic Press, 1995.
13. J. M. Dudley, G. Genty and S. Coen, "Supercontinuum generation in photonic crystal fiber," *Rev. Mod. Phys.*, vol. 78, no. 4, pp. 1135-1184, 2006.

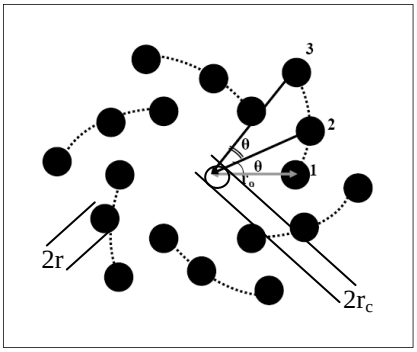

Fig. 1. Schematic of the ES-PCF with defect air-hole at the centre.

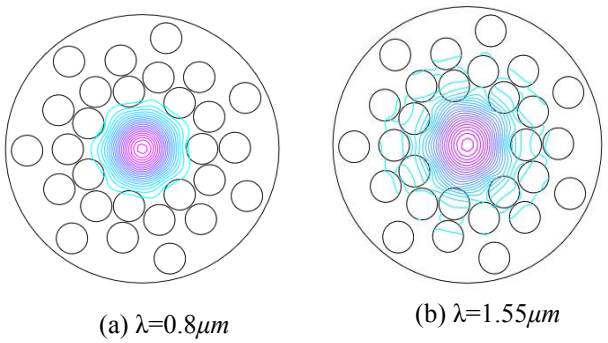

(a) λ=0.8μm (b) λ=1.55μm

Fig. 2. Contour plots of the fundamental modal field in the ES-PCF (not to scale).

Table 1 γ values for the ES-PCF at 1064*nm* and 1550*nm*. *-43944 elements, #-162508 elements, ~-Design B.

$r_c(nm)$	1064*nm*		1550*nm*	
	$\gamma\ (W^{-1}km^{-1})$	$A_{eff}(\mu m^2)$	$\gamma\ (W^{-1}km^{-1})$	$A_{eff}(\mu m^2)$
0*	5585	0.4337	2307	0.7206
0#	5585	0.4337	2307	0.7206
34	5261	0.4604	2177	0.7637
48	5032	0.4814	2065	0.8047
0~	5558	0.4356	2205	0.7536
20~	5426	0.4462	2155	0.7714

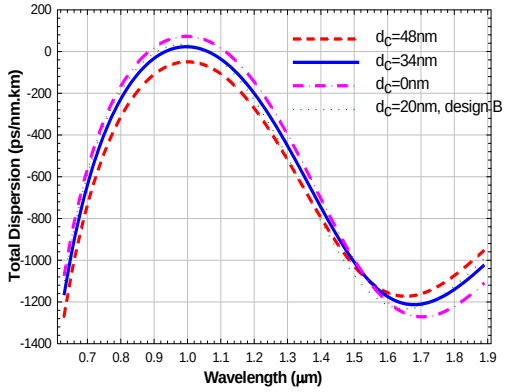

Fig. 3. Dispersion variation with wavelength for the ES-PCF.